

Inhibition of pitting corrosion of C-steel in oilfield-produced water using some purine derivatives

S. Abd El Wanees^{a,b,*}, Arej S. Al-Gorair^c, H. Hawsawi^d, Mohamed T. Alotaibi^e,
Mahmoud G.A. Saleh^f, M. Abdallah^{g,h}, Salah S. Elyanⁱ

^aUniversity Collage of Umlj, University of Tabuk, Tabuk 71491, Saudi Arabia, email: s_nasr@ut.edu.sa

^bChemistry Department, Faculty of Science, Zagazig University, Zagazig, Egypt

^cChemistry Department, College of Science, Princess Nourah Bint Abdulrahman University, Riyadh, Saudi Arabia, email: asalgorir@pnu.edu.sa

^dUniversity College of Alwajh, Alwajh, Tabuk University, Tabuk, Saudi Arabia, email: hnoho60@gmail.com

^eChemistry Department, Turabah University College, Taif University, Saudi Arabia, email: mtotaibi@tu.edu.sa

^fChemistry Department, Faculty of Science, Northern Border University, Arar, Saudi Arabia, email: mgsaleh72@yahoo.com

^gChemistry Department, Faculty of Science, Umm Al-Qura University, Makkah Al Mukaramha, Saudi Arabia, email: metwally555@yahoo.com

^hChemistry Department, Faculty of Science, Banha University, Banha, Egypt

ⁱSchool of Biotechnology, Badr University in Cairo, Badr City, Cairo 11829, email: salah.abosalem1@gmail.com

Received 5 March 2022; Accepted 14 July 2022

ABSTRACT

The pitting corrosion current of C-steel in 50% diluted oilfield-produced water devoid of and containing various amounts of some purine inhibitors, 9H-purine-2,6-diamine, Inh I, 9H-purin-6-amine, Inh II, and 2-amino-1H-purin-6(9H)-one, Inh III was followed under natural corrosion conditions. In the inhibitor-free solution, the pitting corrosion current starts to initiate after an induction period, τ which extends to ~ 40 min and propagates to reach a steady-state current, I_s . In the presence of an inhibitor, the induction period increases with a decrease in the I_s values that depends on the inhibitor type, concentration, and temperature. The surface coverage, θ , and the inhibition efficiency, η , were found to depend on the inhibitor type and its concentration, and decreased with temperature. The inhibition mechanism is supposed to occur through an adsorption process obeying Langmuir's model. The scanning electron microscopy, and energy-dispersive X-ray spectroscopy were used to characterize and analyze the elements of the C-steel surface. Some thermodynamic parameters of the adsorption process such as K_{ads} and ΔG_{ads}° are calculated and discussed.

Keywords: Oilfield-produced water; C-steel; Pitting corrosion; Pitting current; Purine; Inhibition; Adsorption

1. Introduction

C-steel has been used widely in the petroleum field and industrial applications [1,2]. The resistance of this type of steel towards the attack of the aggressive ions, Cl^- , S^{2-} and SO_4^{2-} , in oilfield formation water is very low. The use of the inhibitors is necessary to decrease the pitting attack [2].

Due to the presence of such aggressive ions in the oilfield formation water besides the corrosive dissolved gases like CO_2 and H_2S , corrosion is a serious and big issue in oil and gas production and transportation systems. In addition, it causes an important economic loss to oil and gas producers. The corrosion of the pipe wall frequently causes the failure of oil and gas pipelines [3] resulting in severe economic

* Corresponding author.

losses with environmental pollution [4,5]. Formation water is water trapped in underground formations that are found along with oil or gas. It is considered a by-product or waste stream associated with oil and gas production.

The addition of corrosion inhibitors to oilfield-production water during petroleum output is essential for controlling the destructive effect of different corrosive anions mixed with the produced water environment. Several N-containing organic compounds are used as effective inhibitors for various metals and metal alloys in different electrolytes [6–14]. Safe inhibitors without any polluted effect were chosen as favorable corrosion inhibitors such as 9H-purine-2,6-diamine (Inh I), 9H-purin-6-amine (Inh II), and 2-amino-1H-purin-6(9H)-one, (Inh III) towards the destruction of C-steel in oilfield-production water.

In our study, the influence of the oilfield produced-water obtained from North East Sannan, NES-4, in the Western Desert, Egypt, in a depth of 2,415–2,435 m on the induced pitting corrosion of C-steel was studied. The investigation was carried out by using a simple cell constructed early for measuring the localized pitting corrosion current under natural corrosion conditions in the absence and presence of different concentrations of some purine compounds [15–19]. The surface characterization techniques such as scanning electron microscopy (SEM) and energy-dispersive X-ray spectroscopy (EDX) were used to analyze the surface of unattacked and attacked steel surfaces tested in the aggressive 50% diluted oilfield-produced water in the absence and presence of some purine inhibitors [20].

2. Experimental

2.1. Materials and the electrolytic cell

The required electrodes were prepared from carbon steel C1018. The elemental analysis of these electrodes was estimated, as weight percent, by Tabbin Institute for Metallurgical Studies (TIMS), Helwan–Cairo, Table 1 [21]. The C-steel electrodes were reinforced to Pyrex-glass pipes utilizing an epoxy resin. The free cross-sectional surface area of the prepared electrode required to contact the solution was 0.04 cm². Before each run, the surface area of the steel electrodes was mechanically polished using various grades of polished papers, rinsed with acetone, and finally washed with doubly distilled water.

The pitting corrosion current can be measured utilizing a simple electrolytic cell. This cell is shown diagrammatically in Fig. 1 [21–26]. It consists of a 250 mL borosilicate glass beaker containing 100 cm³ of the examined solution, one of the C-steel electrodes (A), and a magnetic stirrer. The second C-steel electrode (B) was enclosed in a borosilicate glass tube and ended with a fine porosity fritted centered glass disc G₄ (C). The two steel electrodes (A and B) were short-circuited through a nano-ampere meter (Siemens type N-5536).

2.2. Corrosive electrolyte, oilfield-produced water, and inhibitors

Generally, deep oilfield-produced water is liberated in the reservoir rocks before drilling. Such water utilized in our study was gained from one of the wells of the general

petroleum company, GPC, Egypt, in the Western Desert, North East Sannan, NES-4 in a depth of 2415–2435 m underground mixed with crude oil. The chemical composition and physical properties of the produced water are given in Table 2.

The corrosion inhibitor, purine compounds, 9H-purine-2,6-diamine (Inh I), 9H-purin-6-amine (Inh II), and 2-amino-1H-purin-6(9H)-one, (Inh III), Table 3. The utilized organic materials were obtained from Sigma Aldrich chemical company with a purity of 98% and were

Table 1
Elemental analysis C-steel electrodes, C 1018, in wt. %

S	Si	P	Mn	C	Fe
0.60	0.17	0.046	0.50	0.12	Bal 98.564 mass %

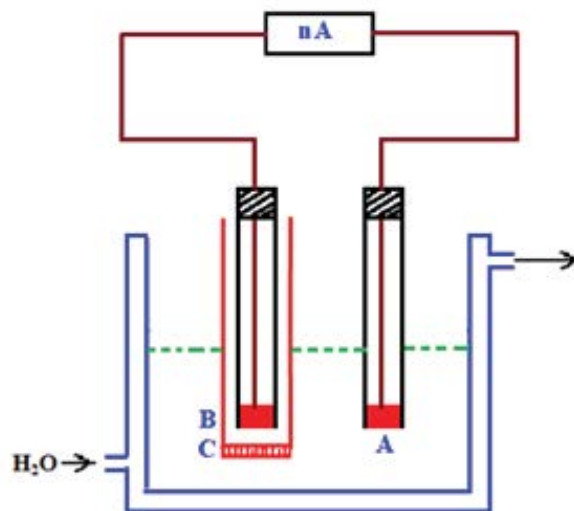
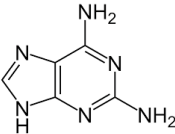
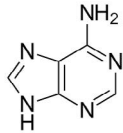
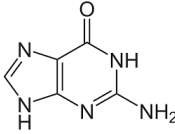


Fig. 1. Electric circuit and electrolytic cell used for pitting corrosion current measurements. A and B are identical C-steel electrodes, C is a fritted centered glass disc G₄ and nA is a nano ampere meters.

Table 2
Physical and chemical characterization of the oilfield-produced water

Character	Unit	Value
pH	Unitless	7.10
Cl ⁻	ppm	41,477
SO ₄ ⁻²	ppm	244
Cl ⁻ /SO ₄ ⁻²	ratio	170:1
Ca ⁺²	ppm	2,525
Mg ⁺²	ppm	122
Conductivity	mS/cm	95.2
Sulfur	%	0.2021
Density	g/cm ³	1.03293, at 25°C
Total dissolved salts (TDS)	g/L	47,600

Table 3
The IUPAC name, chemical structure, chemical formula, and molecular mass of the utilized inhibitors molecules

IUPAC name	Structural formula	Chemical formula	Molecular mass (g/mol)
9H-purine-2,6-diamine (Inh I)		C ₅ H ₆ N ₆	150.14
9H-purin-6-amine (Inh II)		C ₅ H ₅ N ₅	135.13
2-amino-1H-purin-6(9H)-one (Inh III)		C ₅ H ₅ N ₅ O	151.13

used without further purification. The inhibitor concentrations was ranging from 1×10^{-6} M up to 5×10^{-3} M. The examined electrolytes were prepared by utilizing double-distilled water. Experiments were done at room temperature, $25^\circ\text{C} \pm 0.1^\circ\text{C}$, excluding those investigated at various temperatures. The influence of temperature was carried out on 1×10^{-4} M of purine compounds and varied between 293 and 318 K. The cell temperature was monitored by utilizing an ultra-programmable thermostat (U.S.A).

The influence of the corrosive anions (Cl^- , S^{2-} and SO_4^{2-} ions), which are naturally present in the 50% diluted oilfield-produced water on the C-steel electrode on the initiation of the pitting corrosion current was followed against the immersion time. Double-distilled water was used to attain the dilution factor of the oilfield-produced water.

Firstly, the prepared electrodes were immersed in a dilute electrolyte, 0.5% diluted oilfield-produced water. Due to the similarity of the electrodes and the electrolytes, no current could be observed while connecting the steel electrodes through the nano ampere meter [21–26]. In a few experiments, however, small currents were observed to flow, apparently resulting from slight uncontrollable differences in environmental conditions. These currents are decayed in a period of ~30 min. When this condition was established, the investigated amount of the 50% diluted oilfield-produced water is comprised in the main compartment of the electrolytic cell, and the initiated current was followed using a nano ampere meter till reaching the steady current value, I_s [21–26]. The other test was conducted with 50% diluted oilfield-produced water containing various amounts of purine inhibitors, Inh I, Inh II, and Inh III. Each run was done with freshly prepared electrode and with a new portion of the examined solution. To ensure the accuracy of the results, every experiment was repeated two times (similar data are obtained) and the average value of the produced current was taken.

Unattacked and attacked steel surfaces were examined with SEM JSM-F100 coupled EDX, Japan.

3. Results and discussion

3.1. Influence of inhibitor additions on the pitting corrosion current

The corrosion inhibitors are used to control the pitting corrosion of C-steel in 50% diluted oilfield-produced water [21]. In this study, three different types of purines are utilized as inhibitors toward the pitting corrosion induced by the destructive Cl^- , S^{2-} , and SO_4^{2-} ions in the examined solution [21]. The data in Fig. 2 represent the constructed current density time curves of the corroded C-steel electrode in 50% diluted oilfield-produced water devoid of and containing various amounts of Inh I, 9H-purine-2,6-diamine. Analogous curves are fined in the presence of Inh II and Inh III, curves are not shown. It is noteworthy to see that, in the inhibitor-free 50% diluted oilfield-produced water, (curve 1, Fig. 2), the corrosion current starts to initiate after an induction period, τ , which extends to about 40 min (zone A, Fig. 2) followed by a continuous rise in the corrosion current (zone B, Fig. 2) owing to the propagation of the pitting corrosion till reaching a constant value, steady-state current, I_s ($I_s = 123 \mu\text{A}/\text{cm}^2$) (zone C, Fig. 2) [21–26]. The appearance of such a high pitting corrosion current is an indication of the presence of an electrochemical reaction at the C-steel surface due to the oxidation of Fe into Fe^{+2} ions [21,25,26].

When a small amount of 9H-purine-2,6-diamine, Inh I (1×10^{-6} M) is added to the 50% oilfield-produced water, the induction period accompanied by the initiation of the pitting corrosion is elongated ($\tau = 59$ min) with lowering in the steady-state current synchronous to the pitting propagation process ($I_s = 92 \mu\text{A}/\text{cm}^2$). Higher amounts of Inh I (5×10^{-3} M) increase the induction period, τ , to reach 169 min with more lowering in I_s values to reach $11 \mu\text{A}/\text{cm}^2$. Similar behavior is noticed in the case of Inh II and Inh III. Such behavior is related to the passivation of the formed pits by the influence of the inhibitor that can form a protective layer around the C-steel surface decreasing the

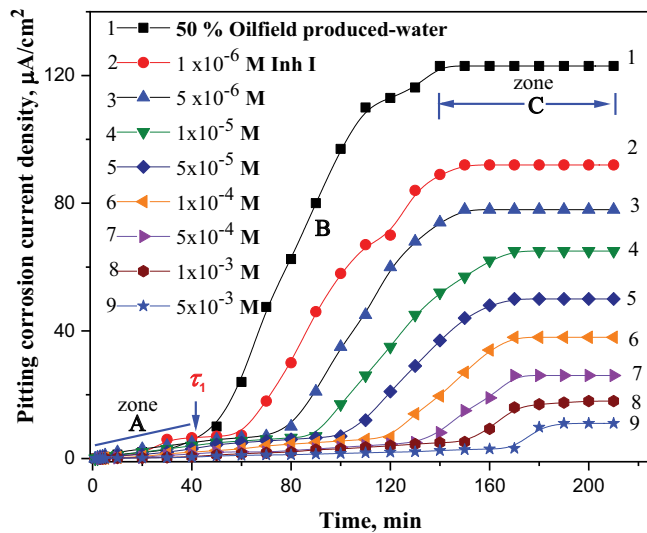


Fig. 2. Current time curves for C-steel immersed in 50% diluted oilfield-produced water, containing various additions of inhibitor I, at 25°C.

corrosion process. This attitude signalizes that the added purine compounds act as good inhibitors toward the pitting corrosion of the C-steel in the oilfield-produced water.

However, the steady rise in the current (zone B, Fig. 2) is due to the initiation of the pitting current with the propagation of the pitting corrosion. The increase in current could be due to the increase in the number of active pits that are formed on the C-steel surface that is harmonizing the raise in the total damaged area [27]. The pitting corrosion current density eventually attains the steady-state value, I_s , that is suppressed by inhibitors and relies on the amount of the inhibitive molecules in the investigated solution. The attainment of the I_s signifies that the produced pitting current of the C-steel surface takes place at the under-most of the created pits without a change in the number of these pits [9,27–31]. The decrease in the steady-state current upon increasing the additions of purine compounds suggests a reduction in the number of the initiated pits, that is, minimized anodic area [27,28].

The dependence of the induction time, τ , on the amount of the added inhibitor (C_{inh}) in 50% oilfield-produced water can be depicted in Fig. 3. The data of such curve performs a logarithmic relation between the two parameters (τ and C_{inh}) that are fulfilling the relation [10–15]:

$$\log \tau = \zeta + \lambda \log C_{inh} \quad (1)$$

where ζ and λ are constants that rely on the nature of the aggressive solution, the type of the investigated inhibitor, and the metal under test [21,23,24,26].

The decrease in the pitting corrosion current density with the purine concentration can be represented by the curves in Fig. 4. This figure represents the variation of the logarithm of the steady-state current, $\log I_s$ with the logarithm of the molar concentration of the inhibitor, $\log C_{inh}$ for purine compounds (Inh I, Inh II, and Inh III). The plots depicted S-shaped curves which could elucidate the promised action of the examined inhibitors to act by an

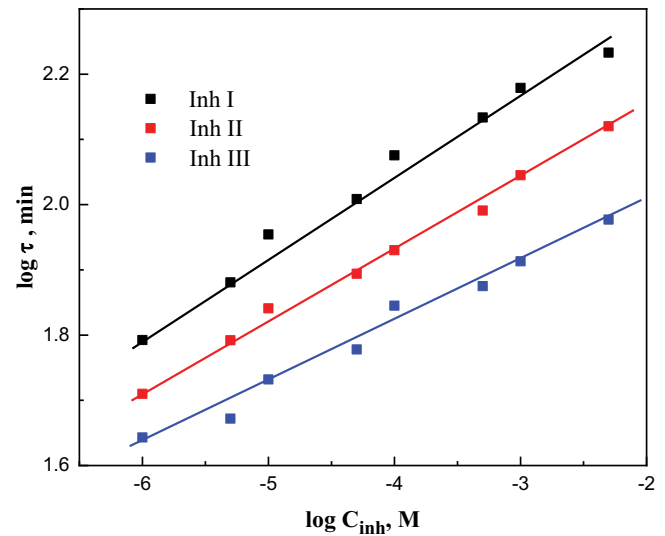


Fig. 3. Variation of the $\log \tau$ against $\log C_{inh}$ for C-steel in 50% diluted oilfield-produced water for different purine compounds, at 25°C.

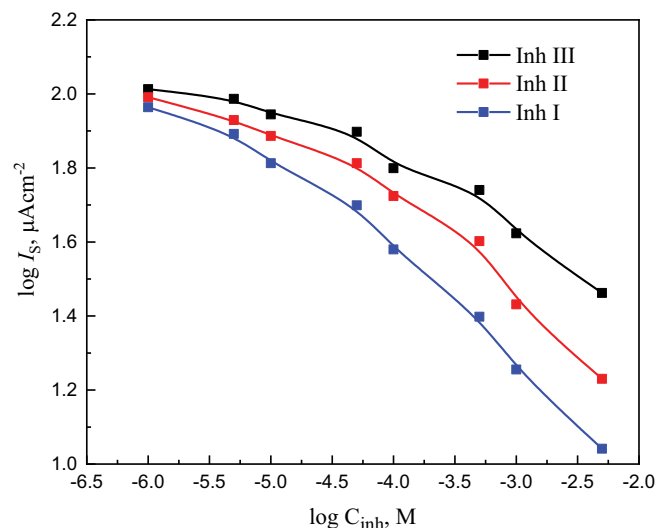


Fig. 4. The $\log I_s - \log C_{inh}$ plots for C-steel immersed in 50% diluted oilfield-produced water, at 25°C.

adsorption process [26,28]. These compounds are supposed to adsorb on the C-steel preventing the aggressive ions, Cl^- , S^{2-} , and SO_4^{2-} to attack the metal surface by forming an adsorbed film, as confirmed later by SEM investigation. The similarity in the S-shaped curves for all purine inhibitors proves that the mitigation of the corrosion process is managed by the same adsorption mechanism [26].

The amplitude of the mitigation towards the localized pitting corrosion on the C-steel by the purine molecules could be estimated from the data of the surface coverage, θ , and the inhibition efficiency, η %. The values of θ and η % (Tables 4 and 5) are deduced from the values of steady-state currents according to Eqs. (2) and (3) [23,24,26].

Table 4

Calculated values of the surface coverage, θ , and inhibition efficiency, η %, for different concentrations of purine inhibitors, on C-steel surface in 50% diluted oilfield-produced water, at 25°C

Conc., M	Inh I		Inh II		Inh III	
	θ	η %	θ	η %	θ	η %
1×10^{-6} M	0.25	25.2	0.20	20.3	0.16	16.3
5×10^{-6} M	0.37	36.6	0.31	30.9	0.21	21.1
1×10^{-5} M	0.47	47.2	0.37	37.4	0.28	28.4
5×10^{-5} M	0.59	59.3	0.47	47.2	0.36	35.8
1×10^{-4} M	0.69	69.1	0.57	56.6	0.44	43.8
5×10^{-4} M	0.80	79.7	0.68	67.5	0.55	55.3
1×10^{-3} M	0.85	85.4	0.78	78.0	0.66	65.9
5×10^{-3} M	0.91	91.1	0.86	86.2	0.76	76.4

Table 5

Calculated values of the surface coverage, θ , and inhibition efficiency, η %, for, on C-steel surface in 50% diluted oilfield-produced water containing 1×10^{-4} M of different purine inhibitors at different temperatures

Temperature, K	Inh I		Inh II		Inh III	
	θ	η %	θ	η %	θ	η %
293	0.70	69.7	0.56	56.0	0.43	42.6
298	0.69	68.9	0.57	56.6	0.44	43.8
303	0.59	59.3	0.54	53.6	0.41	41.1
308	0.55	55.3	0.48	48.4	0.36	36.3
313	0.49	49.0	0.46	45.8	0.37	36.8
318	0.41	41.4	0.36	36.4	0.32	31.8

$$\theta = \left(1 - \frac{I_{s,inh}}{I_{s,free}} \right) \quad (2)$$

$$\eta = \left(1 - \frac{I_{s,inh}}{I_{s,free}} \right) \times 100 \quad (3)$$

where $I_{s,free}$ and $I_{s,inh}$ are the steady-state currents in 50% diluted oilfield-produced water devoid of and containing purine compound, respectively. The calculated values of θ and η % at different amounts of purine compounds are presented in Table 4. Also, Table 5 shows that the values of θ and η % for C-steel in 50% diluted oilfield-produced water containing 0.0001 M of purine inhibitors are reduced with rising the solution temperature. This behavior could be attributed to the desorption of the inhibitor molecules from the metal surface at high temperatures. The increases in the temperature rises the probability of the aggressive ions to attack the C-steel surface and enhancing pitting corrosion [32,33]. Screening of Tables 4 and 5 reveals the following:

- At a constant temperature, the values θ and η % of the added inhibitor are increased with raising the inhibitor concentration.

- The θ and η % values are increased in the order: Inh III < Inh II < Inh I, which is accompanied by the sequence of the inhibition tendency of the added purine against the pitting corrosion of the C-steel.
- At a fixed inhibitor concentration the θ and η % values are decreased as the temperature is increased.
- Inh I is more effective on the C-steel surface than other inhibitors, Inh II, and Inh III. This greatly enhanced the strength of the adsorbed film against the pitting corrosion depend on the number of adsorption sites on the inhibitor molecules.

3.2. Influence of temperature

The influence of temperature on the pitting corrosion of C-steel in 50% diluted oilfield-produced water was investigated without and with the additions of purine compounds. The curves of Fig. 5A and B represent the current-time curves for C-steel immersed in 50% diluted oilfield-produced water without and with 1×10^{-4} M of purine inhibitor, Inh I, respectively. The temperature varied between 293 and 318 K. Similar curves are gained with Inh II and Inh III (curves not shown). It is noticed that the induction period in all examined solutions (without and with inhibitor) preceding the initiation of pitting corrosion decreases with temperature followed by an increase in the pitting current till reaching a steady-state current, I_s [34]. Such attitude could be attributed to the increase in the rate of corrosion of C-steel with temperature due to the rise in the adsorb-ability of the corrosive ions (Cl^- , S^{2-} , and SO_4^{2-} ions) to the C-steel surface which prevents passivation and promotes the dissolution of metals with raising in the I_s values [35,36]. The values of I_s for C-steel surface in oilfield-produced water devoid of and containing 0.0001 M of different purine compounds are plotted against the temperature in Kelvin scale, Fig. 6. The data of this figure depicts that the I_s is increased with temperature in the case of the aggressive and inhibitive solutions confirming that the mechanism of corrosion does not influence by the presence of purine inhibitors although the decrease in the corrosion rate [26].

The data of the curves of Figs. 5 and 6 reveal that:

- The induction period, τ claimed to initiate the localized pitting corrosion current is decreased and the steady-state corrosion current, I_s accompanied by the pit propagation is raised by raising the temperature.
- The increase in the pitting current with the temperature is owing to the enhancement of the oxidation current ($\text{Fe} \rightarrow \text{Fe}^{e^2} + 2e^-$).
- The steady-state corrosion current, I_s is attained after an induction period which is decreased as the temperature is increased. The purine compounds reduce the I_s due to the inhibition process according to the sequence: Inh III < Inh II < Inh I.

Broadly, increasing the temperature for pitting corrosion enhances the initiation of pitting corrosion by reducing the incubation period, τ , and increasing the steady-state pitting corrosion current density, I_s . The Arrhenius relation can be used to deduce the activation energy, E_a for the pitting

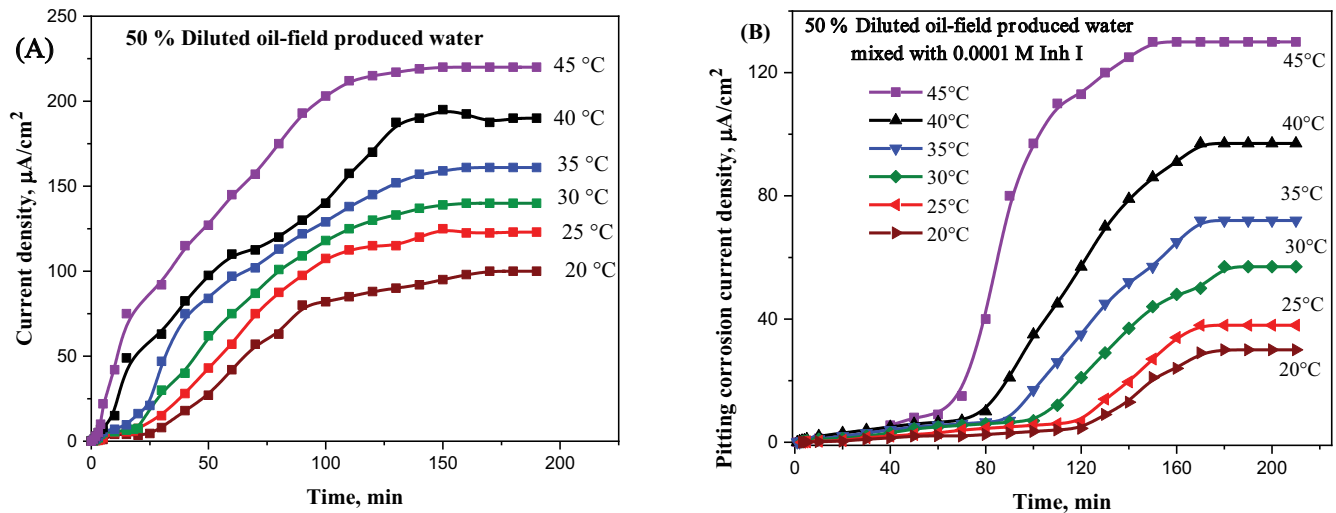


Fig. 5. (A) Current time curves for C-steel in 50% diluted oilfield-produced water, at different temperatures. (B) Current time curves for C-steel in 50% diluted oilfield-produced water mixed with 0.0001 M of Inh I, at different temperatures.

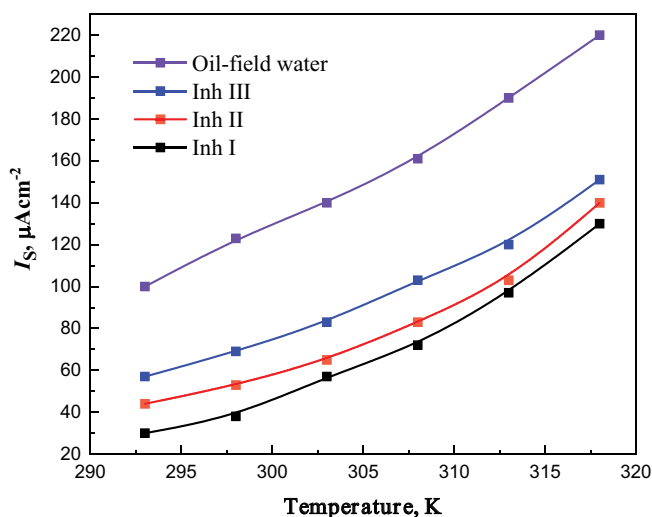


Fig. 6. The plots of the $\log I_s$ – temperature for C-steel in 50% diluted oilfield-produced water containing 0.0001 M of various purine inhibitors.

corrosion reaction [37]. Such an equation can be represented by the following relations [38]:

$$K = A \exp\left(-\frac{E_a}{RT}\right) \quad (4)$$

or

$$\log I_s = \log A - \frac{E_a}{2.303RT} \quad (5)$$

where the rate of reaction (K) can be represented by the I_s values, E_a is the activation energy of the pitting corrosion process, A is the Arrhenius constant, R is the ideal gas constant and T is the absolute temperature.

Fig. 7 depicts the variation of the logarithm of I_s vs. $1/T$ for 50% oilfield-produced water without and with purine inhibitors (1×10^{-4} M). Straight line relations are obtained confirming the Arrhenius relation. The slope of each line can be used to deduce the activation energy, E_a , required for pitting corrosion for all examined electrolytes, Table 6. The calculated value of E_a for the corrosion of C-steel in inhibitor-free 50% diluted oilfield-produced water is less than that obtained in the case of the purine compound solutions. Such behavior could be attributed to the increase in the energy barrier of the inhibitor molecules than those in the oilfield-produced water alone. This confirms that the presence of purine compounds tolerates the pitting corrosion of C-steel in oilfield-produced water due to competing with the aggressive anions to adsorb on the C-steel surface forming a protective layer, lowering the pitting corrosion [39]. The computed E_a accompanying the pitting corrosion increases in the order: of 50% oilfield-produced water < Inh III < Inh II < Inh I. This sequence confirms the variation in the inhibition efficiency of purine compounds which depends on the adsorption sites on each compound. 9H-purine-2,6-diamine (Inh I) is the more effective compound while 2-amino-1H-purin-6(9H)-one (Inh II) is the least.

Other thermodynamic parameters, entropy (ΔS°) and enthalpy (ΔH°) of activation can be deduced when using the transition-state equation [40–47]

$$\log\left(\frac{I_s}{T}\right) = \log\frac{R}{Nh} + \frac{\Delta S^\circ}{2.303R} - \frac{\Delta H^\circ}{2.303RT} \quad (6)$$

where N is the Avogadro's number, R is the universal gas constant, and h is the Planck's constant. Plotting of $\log I_s T^{-1}$ vs. $1/T$ for 50% diluted oilfield-produced water devoid of and containing purine inhibitors (1×10^{-4} M) gives straight-line relations, Fig. 8. The slope of the gained plots represents the value of $\Delta H^\circ/2.303R$ while the intercept is equal to $(\Delta S^\circ/2.303R) + \log(R/Nh)$. The values of ΔH° and ΔS° are computed and tabulated in Table 6. The activation

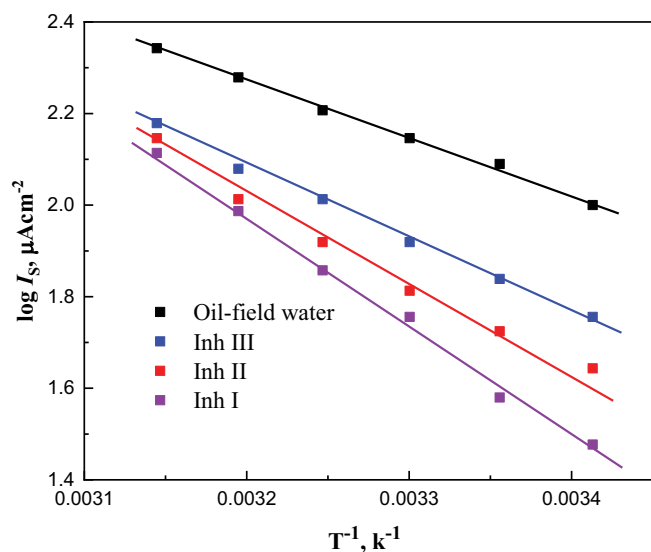


Fig. 7. Arrhenius plots, $\log I_s$ against $1/T$, for C-steel in 50% diluted oilfield-produced water mixed with 0.0001 M of various purine inhibitors.

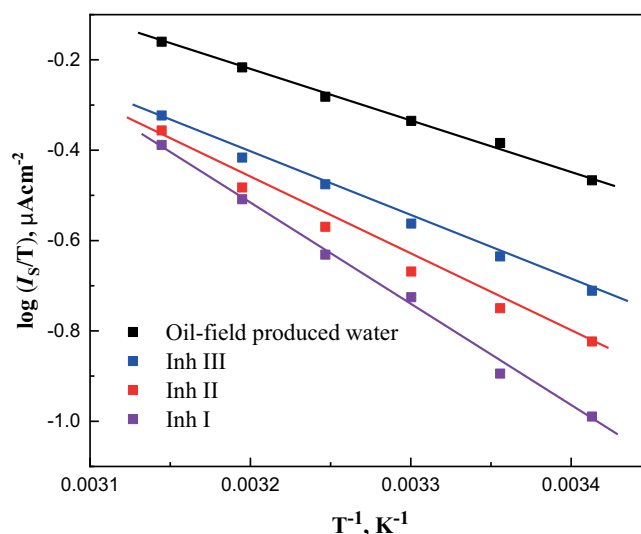


Fig. 8. Transition state plots, $\log(I_s/T)$ against $1/T$, for C-steel in 50% diluted oilfield-produced water without and with 0.0001 M of various purine inhibitors.

Table 6

Thermodynamic corrosion parameters, activation energy for pitting corrosion, E_a , enthalpy of activation, ΔH° , kJ/mol, and entropy of activation, ΔS° , J/mol, and correlation coefficient, R^2 , of purine inhibitors on C-steel surface in 50% diluted oilfield-produced water, at 25°C

Type of solution	E_a , kJ/mol	ΔH° , kJ/mol	ΔS° , J/mol	R^2
50% diluted oilfield-produced water	23.51	21.34	-133	0.996
Inh III	29.86	27.32	-118	0.999
Inh II	35.46	32.91	-101	0.988
Inh I	45.95	43.40	-68	0.996

adsorption entropy ΔS° is determined to be -183 J mol/K for the inhibitor-free 50% diluted oilfield-produced water. In the case of 1×10^{-4} M of purine compound solutions the values of ΔS° are -118 , -101 , and -68 J mol/K for Inh III, Inh II, and Inh I, successively. The negative values of ΔS° for all examined solutions confirm that the activated complex in the rate-determining step represents an association rather than dissociation. Such attitude is due to the reduction in the disordering that takes place [39–43]. The positive values of ΔH° confirm that the transition state process (the activated complex) is endothermic.

3.3. Adsorption isotherm

Generally, the corrosion inhibition of most inhibitor molecules is directly accomplice by an adsorption process [48–51]. Such an adsorption process could follow various models of adsorption isotherms, like Langmuir, Freundlich, Temkin, and Frumkin [52,53]. The surface coverage, θ can be deduced from the steady-state current values, I_s , without and with the presence of inhibitors [26,54].

The obtained values of θ for all used purine compounds confirmed the Langmuir model, Fig. 9. Such an adsorption

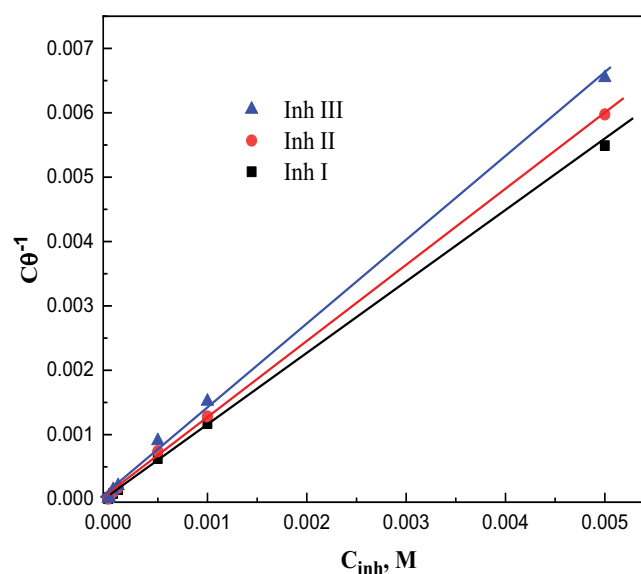


Fig. 9. Langmuir adsorption isotherm for purine inhibitors on C-steel in 50% diluted oilfield-produced water at 25°C.

model can be represented by the following relations [55–57]:

$$\frac{\theta}{1-\theta} = K_{\text{ads}} C_{\text{inh}} \quad (7)$$

Or

$$\frac{C}{\theta} = \frac{1}{K_{\text{ads}}} + C_{\text{inh}} \quad (8)$$

where K_{ads} represents the adsorption–desorption equilibrium constant, and C_{inh} is the equilibrium concentration of the added inhibitor. Fig. 9 depicts straight-line relations between $C_{\text{inh}} \theta^{-1}$ vs. C_{inh} for all added purine compounds with slopes very near to one with correlation coefficients very near to one, Table 7. The adsorption–desorption equilibrium constants, K_{ads} are deduced from the values of the intercept of these straight lines. The K_{ads} data may be considered as a measure of the power of the adsorption of purine compounds on the C-steel surface [57]. The K_{ads} values are found to be 30.4×10^3 , 19.7×10^3 , and $11.2 \times 10^3 \text{ mol}^{-1}$ for Inh I, Inh II, and Inh III, successively. This conclusion approves that Inh I is more effective than Inh II followed by Inh III.

The standard free energy of adsorption, $\Delta G_{\text{ads}}^{\circ}$ can be deduced from the K_{ads} values according to the relation [58–62]

$$K_{\text{ads}} = \frac{1}{55.5} \exp\left(\frac{-\Delta G_{\text{ads}}^{\circ}}{RT}\right) \quad (9)$$

where 55.5 represents the molar concentration of water, R is the universal gas constant and T is the temperature on the Kelvin scale. The calculated values of $\Delta G_{\text{ads}}^{\circ}$ are -35.53 , -34.45 , and -33.05 kJ/mol for Inh I, Inh II, and Inh III, successively. This is proportionate with the higher inhibition efficacy of Inh I followed by Inh II and Inh III. The negative signs of $\Delta G_{\text{ads}}^{\circ}$ confirm the spontaneity of the adsorption process on the C-steel surface with the constancy of the adsorbed film on the C-steel surface. The obtained values of $\Delta G_{\text{ads}}^{\circ}$ are proportionate with a chemisorption process due to coordinate bonds formed between the nitrogen atoms and the Fe atoms on the metal surface [63–66].

3.4. Surface investigation

The SEM micrographs with a magnification of 1,000 times of the C-steel samples before and after immersion for a period of 6 hrs in 50% diluted oilfield-produced water devoid of and containing 0.0001 M inhibitor I are shown in Fig. 10A–C, successively. The micrograph in Fig. 10A (polished C-steel sample) shows that the C-steel surface was smooth and without pits formation. The micrograph of the inhibitor-free 50% diluted oilfield-produced water sample displays a huge number of pits of varying sizes that appear scattered on the surface of the examined area, Fig. 10B, confirming the destructive effect of the oilfield-produced water due to the presence of Cl^- , S^{2-} , and SO_4^{2-} ions. While in the presence of inhibitor I, Fig. 10C, the micrograph offers a less damaged area with a few numbers of more fine pits spreads on the C-surface which confirms the mitigation of the pitting corrosion [21].

Table 7

Adsorption parameters (K_{ads} , mol and $-\Delta G_{\text{ads}}^{\circ}$, kJ/mol) and correlation coefficient, R^2 , of purine inhibitors on C-steel surface in 50% diluted oilfield-produced water, at 25°C

Type of inhibitor	K_{ads} , mol	$\Delta G_{\text{ads}}^{\circ}$, kJ/mol	R^2
Inh I	30.4×10^3	-35.53	0.997
Inh II	19.7×10^3	34.45	0.999
Inh III	11.2×10^3	-33.05	0.998

EDX spectra were used to determine the elements which are present on the C-steel surface before and after exposure to the examined solutions. EDX was carried out to analyze the surface composition of the protective film formed. The EDX spectrum of the polished C-steel sample in Fig. 11A revealed characterized signals for C-steel compositions. The EDX spectrum in the case of the C-steel sample immersed in 50% diluted oilfield-produced water for 6 hr in the absence of the inhibitor revealed characterized signals for C-steel compositions and corrosion products (i.e., O, Cl, Ca, Mg, C, S, and Fe), as shown in Fig. 11B. In the presence of a 0.0001 M inhibitor, the EDX spectrum in Fig. 11C shows that the Fe peak is considerably suppressed relative to the sample in 50% oilfield-produced water with the appearance of new signals. The suppression of the Fe peak and vanishing of Cl signals with the appearance of the N signal would confirm the presence of the overlying inhibitor film on the C-steel surface. This supports that a surface film inhibited the metal dissolution and preventing pitting corrosion. The protective film formed by the inhibitor molecules was strongly adherent to the surface, which leads to a high degree of inhibition efficiency.

Therefore, EDX and SEM examinations of the electrode surface support the experimental data obtained from the chemical method that purine compounds can be regarded as effective inhibitors for corrosion of C-steel in 50% oilfield-produced water.

3.5. Mechanism of inhibition

The corrosion inhibition mechanism is based on the adsorption of the inhibitor molecules on the metal surface in the investigated inhibitive solution. The adsorption mechanism [67] may be due to the electrostatic interaction and/or a coordinate bond formation between the unshared pairs of electrons located on the electronegative atoms on the inhibitor molecules and the Fe atoms on the C-steel surface. The reality that based on the adsorption of inhibitors on the C-steel surface proceeds via chemical adsorption signalize that the inhibition mechanism is consistent with the transferred electron from the inhibitor's molecule to the empty orbital of Fe on the C-steel surface. The adsorbed inhibitor can form a complex with the Fe surface and then protect the metal against further corrosion attacks by blocking the active sites by the N-atoms and heterocyclic rings of the purine inhibitive molecules. The obtained data indicate that Inh I exhibits better performance due to the presence of six nitrogen atoms that are suitable for adsorption besides the presence of the π -electrons of the conjugated system located on the heterocyclic rings which facilitates the adsorption process. So, this compound covers

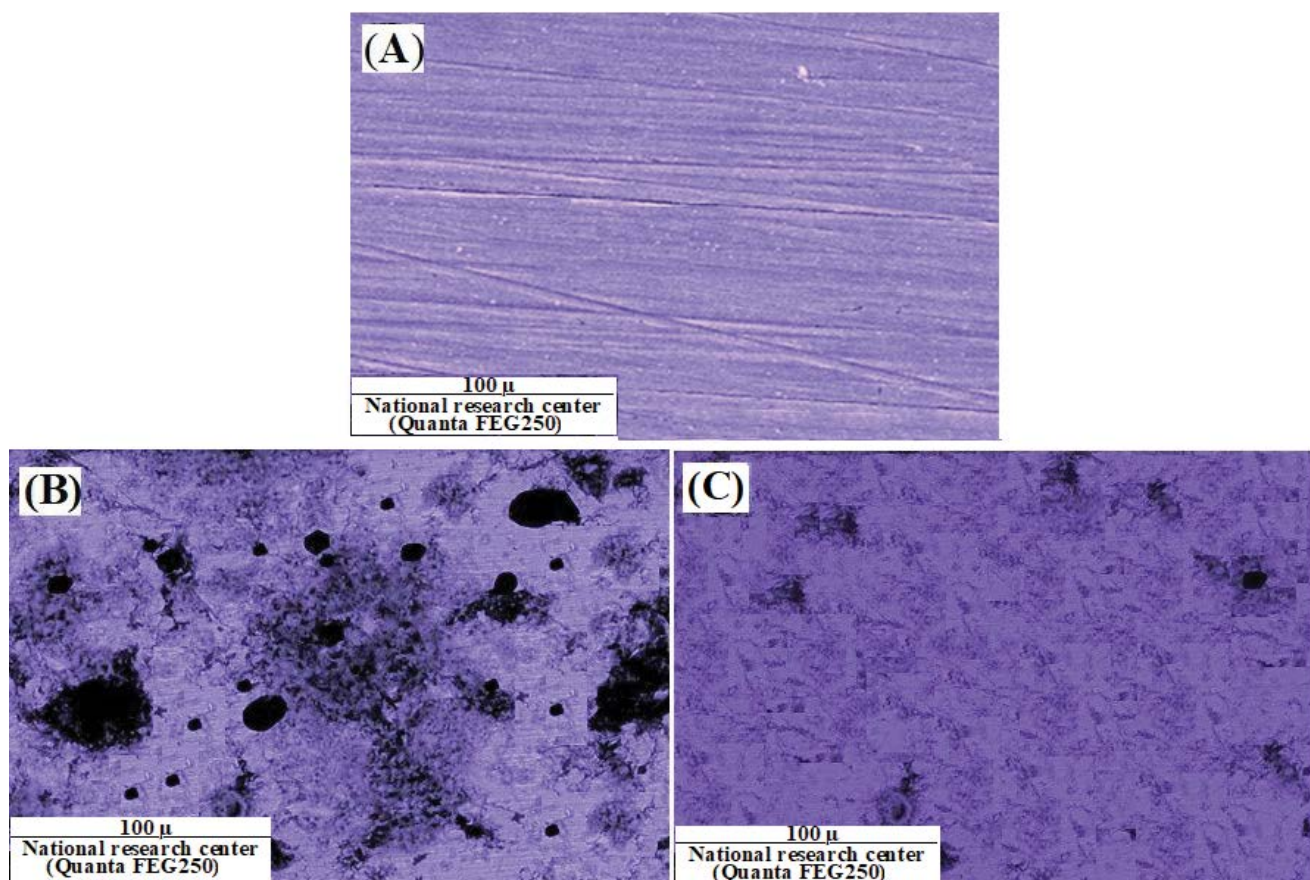


Fig. 10. SEM micrographs with a magnification of 1,000 times of C-steel surface before immersion (A), after immersion for 6 h in 50% diluted oilfield-produced water, without (B), and with 0.0001 M inhibitor I (C), at 25°C.

the C-steel surface and protects it through the lone pairs of electrons located in the active centers, which leads to an increase in the adsorption ability and surface coverage thereby giving higher inhibition efficiency. Inh II exhibits less inhibition efficacy than that Inh I and is more effective than Inh III. This attitude can be attributed to the existence of five nitrogen atoms in addition to the π -electrons of the conjugated system in the heterocyclic rings. Inh III is the least efficient compound which could be attributed to the less number of adsorption centers besides the presence of the inductive effect of the carbonyl group which decreases the electron density on the adsorption centers [68].

4. Conclusions

From measurements of the pitting corrosion current of C-steel in 50% diluted oilfield-produced water in the absence and presence of some purine derivatives the following conclusions could be drawn:

- The pitting corrosion current starts to follow after an induction period that depends on the purine concentration and temperature.
- The induction period required for the initiation of pitting increases with increasing the amount of the added purine.

- The steady-state corrosion current density decreases with increasing purine concentration.
- Raising the temperature decreases the induction period and increases the pitting corrosion current.
- The inhibition efficiency is reduced in the order: Inh I > Inh II > Inh III.
- The activation energy accompanied by the pitting corrosion is increased in the order: Inh III < Inh II < Inh I.

Disclosure statement

The authors declare no potential conflict of interest in preparing this article.

Acknowledgment

The authors express their gratitude to Princess Nourah bint Abdulrahman University Researcher for their support project number (PNURSP2022R94). Princess Nourah bint Abdulrahman University, Riyadh, Saudi Arabia.

References

- [1] A.S. Fouda, A.M. Eldesoky, M.A. Elmorsi, T.A. Fayed, M.F. Atia, New eco-friendly corrosion inhibitors based on phenolic derivatives for protection mild steel corrosion, *Int. J. Electrochem. Sci.*, 8 (2013) 10219–10238.

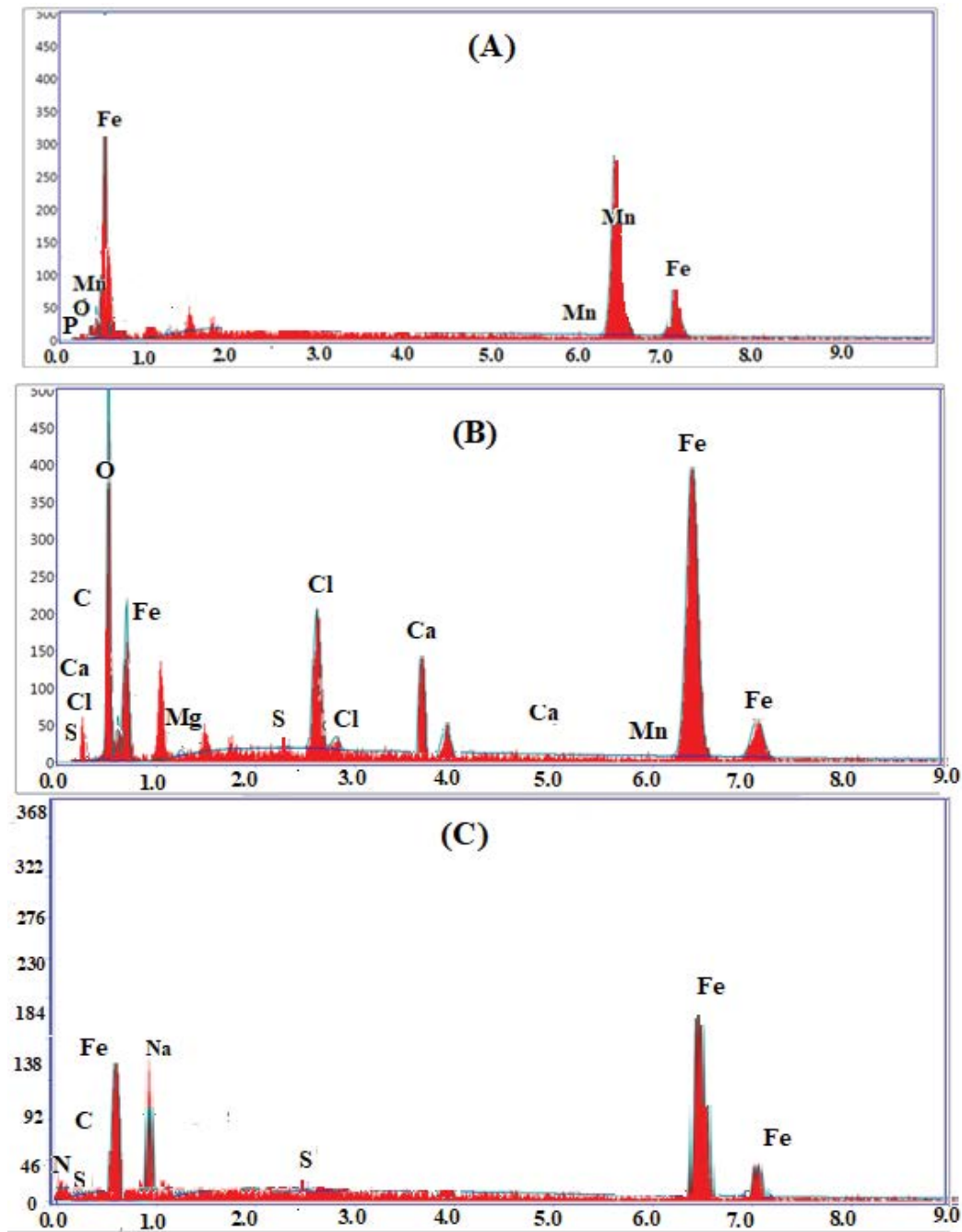


Fig. 11. EDX spectra of C-steel surface before immersion (A), after immersion for 6 h in 50% diluted oilfield-produced water, without (B), and with 0.0001 M inhibitor I (C), at 25°C.

- [2] M.A. Deyab, S.S. Abd El-Rehim, Effect of succinic acid on carbon steel corrosion in produced water of crude oil, *J. Taiwan Inst. Chem. Eng.*, 45 (2014) 1065–1072.
- [3] E. Sadeghi Meresht, T. Shahrabi Farahani, J. Neshati, 2-Butyne-1,4-diol as a novel corrosion inhibitor for API X65 steel pipeline in carbonate/bicarbonate solution, *Corros. Sci.*, 54 (2012) 36–44.
- [4] J. Tang, Y. Shao, T. Zhang, G. Meng, F. Wang, Corrosion behavior of carbon steel in different concentrations of HCl solutions containing H₂S at 90°C, *Corros. Sci.*, 53 (2011) 1715–1723.
- [5] V. Garcia-Arriaga, J. Alvarez-Ramirez, M. Amaya, E. Sosa, H₂S, and O₂ influence on the corrosion of carbon steel immersed in a solution containing 3 M diethanolamine, *Corros. Sci.*, 52 (2010) 2268–2279.
- [6] M.B. Petrović Mihajlović, M.B. Radovanović, A.T. Simonović, Ž.Z. Tasić, M.M. Antonijević, Evaluation of purine-based compounds as the inhibitors of copper corrosion in simulated body fluid, *Res. Phys.*, 14 (2019) 102357, doi: 10.1016/j.rinp.2019.102357.
- [7] Y. Yan, W. Li, L. Cai, B. Hou, Electrochemical and quantum chemical study of purines as corrosion inhibitors for mild steel in 1 M HCl solution, *Electrochim. Acta*, 53 (2008) 5953–5960.
- [8] Q.H. Zhang, B.S. Hou, N. Xu, W. Xiong, H.F. Liu, G.A. Zhang, Effective inhibition on the corrosion of X65 carbon steel in

- the oilfield-produced water by two Schiff bases, *J. Mol. Liq.*, 285 (2019) 223–236.
- [9] S. Abd El Wanees, Amines as inhibitors for corrosion of copper in nitric acid, *Anti-Corros. Methods Mater.*, 41 (1994) 3–7.
- [10] Z. Jiang, Y. Li, Q. Zhang, B. Hou, W. Xiong, H. Liu, G. Zhang, Purine derivatives as high efficient eco-friendly inhibitors for the corrosion of mild steel in acidic medium: experimental and theoretical calculations, *J. Mol. Liq.*, 32 (2021) 114809, doi: 10.1016/j.molliq.2020.114809.
- [11] K. Zakaria, A.A. Farag, Thermodynamic and adsorption behavior of eco-friendly purine derivatives on the corrosion of carbon steel in 1 M HCl, *Int. J. Sci. Res.*, 3 (2014) 1092–1099.
- [12] X.H. Li, S.D. Deng, H. Fu, T.H. Li, Adsorption and inhibition effect of 6-benzyl amino purine on cold-rolled steel in 1.0 M HCl, *Electrochim. Acta*, 54 (2009) 4089–4098.
- [13] X. Wang, J. Xu, C. Sun, M.C. Yan, Effect of oilfield produced water on corrosion of pipeline, *Int. J. Electrochem. Sci.*, 10 (2015) 8656–8667.
- [14] M. Askari, M. Aliofkhaezrai, R. Jafari, P. Hamghalam, A. Hajizadeh, Downhole corrosion inhibitors for oil and gas production – a review, *Appl. Surf. Sci. Adv.*, 6 (2021) 100128, doi: 10.1016/j.apsadv.2021.100128.
- [15] S.M. Shaban, E. Badr, M.A. Shenashen, A.A. Farag, Fabrication and characterization of encapsulated Gemini cationic surfactant as anticorrosion material for carbon steel protection in down-hole pipelines, *Environ. Technol. Innovation*, 23 (2021) 101603, doi: 10.1016/j.eti.2021.101603.
- [16] S.M. Shaban, M.F. Elbhrawy, A.S. Fouda, S.M. Rashwan, H.E. Ibrahim, A.M. Elsharif, Corrosion inhibition and surface examination of carbon steel 1018 via N-(2-(2-hydroxyethoxy) ethyl)-N,N-dimethyloctan-1-aminium bromide in 1.0 M HCl, *J. Mol. Struct.*, 1227 (2021) 129713, doi: 10.1016/j.molstruc.2020.129713.
- [17] S.M. Shaban, A. Saied, S.M. Tawfik, A. Abd-Elaal, I. Aiad, Corrosion inhibition and biocidal effect of some cationic surfactants based on Schiff base, *J. Ind. Eng. Chem.*, 19 (2013) 2004–2009.
- [18] A.A. Taha, S.M. Shaban, H.A. Fetouh, S.T. Taha, V.M. Sabet, D.-H. Kim, Synthesis and evaluation of nonionic surfactants based on dimethylamino-ethylamine: electrochemical investigation and theoretical modeling as inhibitors during electro polishing in ortho-phosphoric acid, *J. Mol. Liq.*, 328 (2021) 115421, doi: 10.1016/j.molliq.2021.115421.
- [19] A.A. Abd-Elaal, S.M. Shaban, S.M. Tawfik, Three gemini cationic surfactants based on polyethylene glycol as effective corrosion inhibitor for mild steel in acidic environment, *J. Assoc. Arab Univ. Basic Appl. Sci.*, 24 (2017) 54–65.
- [20] K.A. Alamry, M.A. Hussein, A. Musa, K. Haruna, T.A. Saleh, The inhibition performance of a novel benzenesulfonamide-based benzoxazine compound in the corrosion of X60 carbon steel in an acidizing environment, *RSC Adv.*, 11 (2021) 7078–7095.
- [21] S. Abd El Wanees, M.M. Kamel, S.M. Rashwan, Y. Atef, M.G. Abd Elsadek, Inhibition of pitting corrosion on C-steel in oilfield-produced water under natural corrosion conditions, *Desal. Water Treat.*, 248 (2022) 28–38.
- [22] A.M. Shams El Din, S.M. Abd El Haleem, J.M. Abd El Kader, Studies on the pitting corrosion of zinc in aqueous solutions II. Measurement of pitting corrosion currents operating under natural conditions, *J. Electroanal. Chem.*, 65 (1975) 335–349.
- [23] S. Abd El Wanees, A.A. Mohamed, M. Abd El Azeem, A.N.A. El Fatah, Pitting corrosion currents of tin concerning the concentration of the inhibitive and corrosive anions under natural corrosion conditions, *Int. J. Electrochem. Sci.*, 3 (2008) 1005–1015.
- [24] S. Abd El Wanees, A.B. Radwan, M.A. Alsharif, S.M. Abd El Haleem, Initiation and inhibition of pitting corrosion on reinforcing steel under natural corrosion conditions, *Mater. Chem. Phys.*, 190 (2017) 79–95.
- [25] E.E. Abd El Aal, S. Abd El Wanees, A. Diab, S.M. Abd El Haleem, Environmental factors affecting the corrosion behavior of reinforcing steel III. Measurement of pitting corrosion currents of steel in $\text{Ca}(\text{OH})_2$ solutions under natural, *Corros. Sci.*, 51 (2009) 1611–1618.
- [26] S.M. Abd El Haleem, S. Abd El Wanees, E.E. Abd El Aal, A. Diab, Environmental factors affecting the corrosion behavior of reinforcing steel. IV. Variation in the pitting corrosion current concerning the concentration of the aggressive and the inhibitive anions, *Corros. Sci.*, 52 (2010) 1675–1683.
- [27] S. Abd El Wanees, A. Abd El Aal, E.E. Abd El Aal, Effect of polyethylene glycol on pitting corrosion of cadmium in alkaline solution, *Br. Corros. J.*, 28 (1993) 222–228.
- [28] M. Cohen, The Passivity and Breakdown of Passivity of Iron, R.P. Frankeuthal, J. Kurager, N.J. Princiator, Eds., *Passivity of Metals*, The Electrochemical Society, Pennington, NJ, 1978, pp. 521–545.
- [29] S.M. Abd El Haleem, A. Abd El Aal, Pitting corrosion currents on steel in relation to the concentration of the inhibitive and corrosive anions under natural corrosion conditions, *Br. Corros. J.*, 14 (1979) 226–230.
- [30] S.M. Abd El Haleem, A. El Kot, A.A. Abdel Fattah, W. Taylor, Variation of pitting corrosion on Fe surface, *Corros. Preven. Control*, 33 (1986) 151–157.
- [31] E.E. Abd El Aal, Measurements of pitting corrosion currents of zinc in near-neutral media, *Corros. Sci.*, 44 (2002) 2041–2053.
- [32] S.M. Abd El Haleem, E.E. Abd El Aal, S. Abd El Wanees, A. Diab, Environmental factors affecting the corrosion behaviour of reinforcing steel: I. The early stage of passive film formation in $\text{Ca}(\text{OH})_2$ solutions, *Corros. Sci.*, 52 (2010) 3875–3882.
- [33] S. Abd El Wanees, A.A.H. Bukhari, N.S. Alatawi, S.A. Khalil, S. Nooh, S.K. Mustafa, S.S. Elyan, Thermodynamic and adsorption studies on the corrosion inhibition of Zn by 2,2'-dithiobis(2,3-dihydro-1,3-benzothiazole) in HCl solutions, *Egypt. J. Chem.*, 64 (2021) 547–559.
- [34] D.E. Williams, C. Westcott, M. Fleischmann, Studies of the initiation of pitting corrosion on stainless steels, *J. Electroanal. Chem.*, 180 (1984) 549–564.
- [35] Y. Zuo, S. Fu, The effect of potential on metastable pitting of amorphous Ni alloy, *Corros. Sci.*, 39 (1997) 465–471.
- [36] E.E. Abd El Aal, S. Abd El Wanees, Galvanostatic study of the breakdown of Zn passivity by sulphate anions, *Corros. Sci.*, 51 (2009) 1780–1788.
- [37] S. Abd El Wanees, A.S. Al-Gorair, H. Hawsawi, S.S. Elyan, M. Abdallah, Investigation of anodic behavior of nickel in H_2SO_4 solutions using galvanostatic polarization technique. II. Initiation and inhibition of pitting corrosion by some inorganic passivators, *Int. J. Electrochem. Sci.*, 16 (2021) 210548, doi: 10.20964/2021.05.25.
- [38] S. Abd El Wanees, S.H. Seda, Corrosion inhibition of zinc in aqueous acidic media using a novel synthesized Schiff base – an experimental and theoretical study, *J. Dispersion Sci. Technol.*, 40 (2019) 1813–1826.
- [39] S.M. Abd El-Haleem, S. Abd El-Wanees, A. Bahgat, Environmental factors affecting the corrosion behavior of reinforcing steel. V. Role of chloride and sulfate ions in the corrosion of reinforcing steel in saturated $\text{Ca}(\text{OH})_2$ solutions, *Corros. Sci.*, 75 (2013) 1–15.
- [40] S. Abd El Wanees, N.M. El Basiony, A.M. Al-Sabagh, M.A. Alsharif, S.M. Abd El Haleem, M.A. Migahed, Controlling of H_2 gas production during Zn dissolution in HCl solutions, *J. Mol. Liq.*, 248 (2017) 943–952.
- [41] A.S. Al-Gorair, S. Abd El Wanees, H. Hawsawi, M.G.A. Saleh, M. Abdallah, Investigation of the anodic behavior of nickel in H_2SO_4 solutions using galvanostatic polarization technique. III. Inhibition of pitting corrosion using nitrogen-containing organic compounds, *Desal. Water Treat.*, 244 (2021) 147–156.
- [42] M.G.A. Saleh, S. Abd El Wanees, S.K. Mustafa, Dihydropyridine derivatives as controllers for production of hydrogen during zinc dissolution, *Chem. Eng. Commun.*, 206 (2019) 789–803.
- [43] M. Abdallah, A. Fawzy, H. Hawsawi, R.S.A. Hameed, S.S. Al-Juaid, Estimation of water-soluble polymers (poloxamer and pectin) as corrosion inhibitors for carbon steel in acidic medium, *Int. J. Electrochem. Sci.*, 15 (2020) 8129–8144.

- [44] S.K. Shukla, M.A. Quraishi, 4-Substituted aminomethyl propionate: new and efficient corrosion inhibitors for mild steel in hydrochloric acid solution, *Corros. Sci.*, 51 (2009) 1990–1997.
- [45] S. Abd El Wanees, S. Nooh, A. Farouk, S.M. Abd El Haleem, Corrosion inhibition of aluminum in sodium hydroxide solutions using some inorganic anions, *J. Dispersion Sci. Technol.*, (2021) 1914647, doi: 10.1080/01932691.2021.1914647.
- [46] S. Abd El Wanees, A.A. Keshk, Investigation of anodic behavior of nickel in H_2SO_4 solutions using galvanostatic polarization technique. IV. Initiation and inhibition of pitting corrosion by Cl^- ions and ethoxylated surfactants, *Int. J. Electrochem. Sci.*, 16 (2021) 21087, doi: 10.20964/2021.08.38.
- [47] S. Abd El Wanees, A. Diab, O. Azazy, M. Abd El Azim, Inhibition effect of N-(pyridin-2-yl-carbamothioyl) benzamide on the corrosion of C-steel in sulfuric acid solutions, *J. Dispersion Sci. Technol.*, 35 (2014) 1571–1580.
- [48] S.A.M. Refaey, F. Taha, A.M. Abd El-Malak, Corrosion and inhibition of 316L stainless steel in a neutral medium by 2-mercaptobenzimidazole, *Int. J. Electrochem. Sci.*, 1 (2006) 80–91.
- [49] M. Abdallah, A.S. Al-Gorair, A. Fawzy, H. Hawsawi, R.S. Abdel Hameed, Enhancement of adsorption and anticorrosion performance of two polymeric compounds for the corrosion of SABIC carbon steel in hydrochloric acid, *J. Adhes. Sci. Technol.*, 36 (2022) 35–53.
- [50] A.S. Al-Gorair, M. Abdallah, Expired paracetamol as corrosion inhibitor for low carbon steel in sulfuric acid. Electrochemical, kinetics and thermodynamics investigation, *Int. J. Electrochem. Sci.*, 16 (2021) 210771, doi: 10.20964/2021.07.73.
- [51] M. Abdallah, R. El-Sayed, A. Meshabi, M. Alfakeer, Synthesis of nonionic surfactants containing five-membered ring and application as anti-corrosion for the corrosion of carbon steel in 0.5 M H_2SO_4 solution, *Prot. Met. Phys. Chem.*, 57 (2021) 389–397.
- [52] F. Banteiss, M. Traisnel, M. Largrenes, The substituted 1,3,4-oxadiazoles: a new class of corrosion inhibitors of mild steel in acidic medium, *Corros. Sci.*, 42 (2002) 127–146.
- [53] P. Morales Gil, G. Negron-Silva, M. Romero-Romo, C. Angeles-Chavez, M. Paloma-Pardave, Corrosion inhibition of pipeline steel grade API 5L X52 immersed in 1 M H_2SO_4 aqueous solution using heterocyclic organic molecules, *Electrochim. Acta*, 49 (2004) 4733–4741.
- [54] E.E. Abd El Aal, S. Abd El Wanees, Corrosion control of lead in hydrochloric acid solutions by N-phenylcinnamimide and some of its derivatives, *Corrosion*, 67 (2011) 075003–0750012.
- [55] S. Abd El Wanees, M.I. Alahmdi, M. Abd El Azzem, H.E. Ahmed, 4,6-Dimethyl 2-oxo-1,2-dihydropyridine-3-carboxylic acid as an inhibitor towards the corrosion of C-steel in acetic acid, *Int. J. Electrochem. Sci.*, 11 (2016) 448–3466.
- [56] S. Abd El Wanees, S. Nooh, A. Farouk, S.M. Abd El Haleem, Corrosion inhibition of aluminum in sodium hydroxide solutions using some inorganic anions, *J. Dispersion Sci. Technol.*, (2021) 1–16.
- [57] M.A. Amin, Weight loss, polarization, electrochemical impedance spectroscopy, SEM and EDX studies of the corrosion inhibition of copper in aerated NaCl solutions, *J. Appl. Electrochem.*, 36 (2006) 215–226.
- [58] S. Abd El Wanees, M.I. Alahmdi, S.M. Rashwan, M.M. Kamel, M.G. Abd Elsadek. Inhibitive effect of cetyltriphenylphosphonium bromide on C-steel corrosion in HCl solution, *Int. J. Electrochem. Sci.*, 11 (2016) 9265–9281.
- [59] S. Abd El Wanees, E.E. Abd El Aal, N-Phenylcinnamimide and some of its derivatives as inhibitors for corrosion of lead in HCl solutions, *Corros. Sci.*, 52 (2010) 338–344.
- [60] K. Harun, T.A. Saleh, N,N'-Bis-(2-aminoethyl)piperazine functionalized graphene oxide (NAEP-GO) as an effective green corrosion inhibitor for simulated acidizing environment, *J. Environ. Chem. Eng.*, 9 (2021) 104967, doi: 10.1016/j.jece.2020.104967.
- [61] K. Harun, T.A. Saleh, M.A. Quraish, Expired metformin drug as green corrosion inhibitor for simulated oil/gas well acidizing environment, *J. Mol. Liq.*, 315 (2020) 113716, doi: 10.1016/j.molliq.2020.113716.
- [62] K.A. Alawi Al-Sodani1, M. Maslehuddin, O.S. Baghabr Al-Amoudi, T.A. Saleh, M. Shameem, Efficiency of generic and proprietary inhibitors in mitigating corrosion of carbon steel in chloride-sulfate environments, *Sci. Rep.*, 8 (2018) 11443, doi: 10.1038/s41598-018-29413-7.
- [63] E. Stupnišek-Lisac, A. Gazivoda, M. Madžarac, Evaluation of non-toxic corrosion inhibitors for copper in sulphuric acid, *Electrochim. Acta*, 47 (2002) 4189–4194.
- [64] B.B. Damaskin, O.A. Petrii, V. Batrakov, Adsorption of Organic Compounds on Electrodes, Vol. 85, Plenum Press, New York, 1971, p. 499.
- [65] F.E. Heakal, AM. Fekry, Experimental and theoretical study of uracil and adenine inhibitors in Sn-Ag alloy/nitric acid corroding system, *J. Electrochem. Soc.*, 155 (2008) C534–C542.
- [66] M.G.A. Saleh, S. Abd El Wanees, 2,2'-Dithiobis(2,3-dihydro-1,3-benzothiazole) as an effective inhibitor for carbon steel protection in acid solutions, *Desal. Water Treat.*, 265 (2022) 1–11.
- [67] A.O. Alnajara, H.M. Abd El-Lateef, A novel approach to investigate the synergistic inhibition effect of nickel phosphate nanoparticles with quaternary ammonium surfactant on the Q235-mild steel corrosion: surface morphology, electrochemical-computational modeling outlines, *J. Mol. Liq.*, 337 (2021) 116–125.
- [68] A.A. Al-Amiery, A.B. Mohamad, A.A.H. Kadhum, L.M. Shaker, W.N.R.W. Isahak, M.S. Takrif, Experimental and theoretical study on the corrosion inhibition of mild steel by nonanedioic acid derivative in hydrochloric acid solution, *Sci. Rep.*, 12 (2022) 4705, doi: 10.1038/s41598-022-08146-8.